View metadata, citation and similar papers at core.ac.uk
brought to you by CORE
provided by DigitalCommons@USU

Electronic structure and bonding in metal porphyrins, metal=Fe, Co, Ni, Cu, Zn

Meng-Sheng Liao and Steve Scheiner[a)]
Department of Chemistry and Biochemistry, Utah State University, Logan, Utah 84322-0300

(Received 3 January 2002; accepted 2 April 2002)

A systematic theoretical study of the electronic structure and bonding in metal *meso*-tetraphenyl porphines MTPP, M=Fe, Co, Ni, Cu, Zn has been carried out using a density functional theory method. The calculations provide a clear elucidation of the ground states for the MTPPs and for a series of $[\mathrm{MTPP}]^x$ ions ($x=2+, 1+, 1-, 2-, 3-, 4-$), which aids in understanding a number of observed electronic properties. The calculation supports the experimental assignment of unligated FeTPP as $^3A_{2g}$, which arises from the configuration $(d_{xy})^2(d_{z^2})^2(d_{xz})^1(d_{yz})^1$. The calculated M–TPP binding energies, ionization potentials, and electron affinities are in good agreement with available experimental data. The influence of axial ligands and peripheral substitution by fluorine are in accord with the experimental observation that not only half-wave potentials ($E_{1/2}$) of electrode reactions, but also the site of oxidation/reduction, may be dependent on the porphyrin basicity and the type of axial ligand coordination. © *2002 American Institute of Physics.*
[DOI: 10.1063/1.1480872]

I. INTRODUCTION

There has been much interest in the electronic structure of porphyrins and related compounds. This interest stems in part from their biological significance and catalytic properties.[1,2] The biologically important porphyrin derivatives are all metal porphyrins, principally iron. Metal porphyrins have also received much attention in connection with their intrinsically interesting spectroscopic, magnetic, and electrochemical properties. The last decades have witnessed an explosion of experimental studies of metal porphyrins which have yielded very useful information about their electronic structure and optical spectra, but it has not always been possible to provide a well reasoned explanation of the results obtained.

With their high molecular symmetry (square-planar D_{4h}), metal porphyrins are also of considerable theoretical interest in their own right. Few large molecules have enjoyed such popularity among theorists. Very early theoretical studies of porphyrins were limited to semiempirical methods[3] which were able to explain some features of the optical spectra, but required the use of adjustable parameters. The first *ab initio* calculation was done by Almlöf on free-base porphine with minimal basis sets.[4] Later, a number of *ab initio*,[5–11] discrete variational X_α,[12] multiple scattering X_α (MS-Xα),[13] INDO-SCF/CI,[14] and density functional theory[15–20] calculations were carried out in order to explore the electronic and other observed properties of metal porphyrins. Nonetheless, in spite of a large amount of experimental and theoretical data, there are still many unknowns regarding the structural, electronic, and bonding properties for various metal porphyrins, and many fine details remain to be elucidated.

One of the striking features of metal porphyrins is their ability to undergo facile reduction and oxidation; indeed redox processes involving metal porphyrins play a critical role in living systems.[21] Yet the electronic structures of the resulting species remain unclear. Successive formation of mono-, di-, tri-, and tetra-negative ions has been observed for a number of porphyrins and their metal complexes.[22,23] Copper porphyrins, for example, may be reduced by as many as seven electrons,[24] and a variety of metal porphyrins undergo two successive one-electron oxidations.[25] Irikura and Beauchamp[26] have generated a wide variety of both cationic and anionic metal porphyrin ions in the gas phase. However, the character of the acceptor orbitals is poorly understood[27] as is the nature of oxidized species, i.e., whether it is in fact the metal or ligand that is oxidized. For instance, the suggestion that Fe(III) porphyrins can be oxidized to a Fe(IV) species is neither confirmed nor refuted by electrochemical experiments.[28] Correct assignment of the ground states for a series of metal porphyrin ions is rather difficult experimentally, and theoretical studies of this aspect are clearly warranted.

What is the influence of axial ligands on the electronic structure of metal porphyrins? It is known that axial ligation has a substantial influence on the redox[21,24,29] and photovoltaic[30] properties of metal porphyrins. Iron porphyrins with coordinating axial ligands are diamagnetic ($S=0$),[24] in contrast to the four coordinate species ($S=1$). The elucidation of the electronic structure of metal porphyrins with axial ligands is also important for understanding their biological and catalytic functions.

The electronic structure of the porphyrin ring is subject to a number of influences, one of which arises from peripheral substituents. Ghosh *et al.*[31] have performed *ab initio* (Hartree–Fock) and local density functional studies of substituent effects on a series of free-base porphyrins, mainly devoted to ionization potentials, but little is known about the

[a)]Electronic mail: scheiner@cc.usu.edu

 © 2002 American Institute of Physics

Downloaded 13 Jun 2011 to 129.123.124.169. Redistribution subject to AIP license or copyright; see http://jcp.aip.org/about/rights_and_permissions

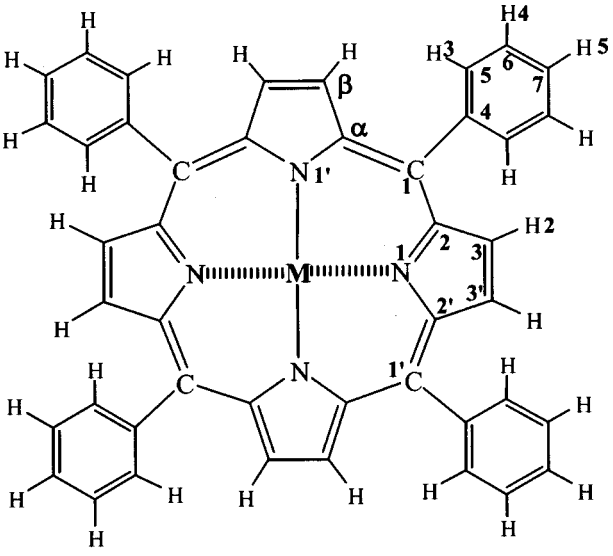

FIG. 1. Atomic numbering schemes of (a) MTPP and (b) MP.

effects of peripheral substitution on the electronic structure and properties of metal porphyrins.

This work represents a systematic theoretical study of the electronic structure and bonding in a series of metal porphyrins using a DFT method. Five complexes of *meso*-tetraphenyl porphines, with first-row transition metals from Fe to Zn, are chosen. The metal *meso*-tetraphenyl porphines [MTPP in Fig. 1(a)] are examined first because a great deal of experimental information is available. All previous high-level *ab initio* and DFT calculations on metal porphyrins considered only the unsubstituted metal porphine (MP) system, whereas a number of different groups (methyl, vinyl, etc.) are found on the periphery of the porphyrin ring in the naturally occurring hemes. Some of the systems that have been synthesized have as substituents phenyl and ethyl, which may have some alternate effects on the properties of metal porphyrins. Since porphine can be regarded as the parent molecule of the porphyrins, calculated results for the MP model systems are presented for the sake of comparison.

II. COMPUTATIONAL METHODS

Quantum chemical calculations were carried out using the Amsterdam density functional (ADF) program package developed by Baerends and co-workers.[32] This formalism uses an expansion of molecular orbitals in atomic-centered STO basis sets, and the atomic core orbitals are calculated at the Dirac–Slater level, then frozen and transferred to the molecular calculation. Relativistic valence-shell effects are calculated quasirelativistically.[33] A number of exchange-correlation potential functionals are included in the suite of programs, and these may be combined to form various functionals. A frozen-core approximation was employed.

The density functional used was based on the Vosko–Wilk–Nusair (VWN) local spin-density potential[34] plus Becke's (B) gradient correction for exchange,[35] and Perdew's (P) gradient correlation for correlation.[36] It has been shown that this VWN–B–P functional can provide accurate bond energies for both main group and transition metal systems.[37] There is also evidence that the energies and topologies of molecular orbitals calculated by DFT methods provide useful information,[16–18,38] comparable to conventional *ab initio* molecular orbitals.

Large triple-zeta STO basis sets were used for the metal $3s$, $3p$, $3d$, and $4s$, C/N $2s-2p$, and H $1s$ valence shells, single-ζ STOs for core orthogonalization. Polarization functions were added to the valence basis sets: one $4p$-type function for the metal, one $3d$-type for C/N, and one $2p$-type for H. The $1s^2 2s^2 2p^6$ configuration on the metals and $1s^2$ configuration on C/N were assigned to the core and kept frozen. For the open-shell states, the unrestricted Hartree–Fock spin-density functional approach was used.

III. RESULTS AND DISCUSSION

A. Structures

The molecular structures and atomic numbering schemes of MTPP and MP are presented in Fig. 1. While the metal porphines exhibit a nearly planar D_{4h} structure,[39] the larger MTPP appears to undergo certain ruffling distortions in the crystal, depending upon the identity of the metal. Monoclinic ZnTPP, for example, belongs to the D_{4h} point group[40] whereas NiTPP adopts the classical S_4 ruffling.[41] It is logical to presume that these different structures are not too dissimilar in energy since, for example, H_2TPP crystallizes in both the triclinic form with an effectively planar macrocycle (D_{2h}) and tetragonal in which the macrocycle is distorted into C_{2v} symmetry.[42]

To further probe the influence of ruffling on the properties of the MTPPs, NiTPP was taken as a prototype, and its geometry was optimized under both D_{4h} and S_4 point group restrictions. The optimized structures are illustrated in Fig. 6, which underscores the arrangements of the peripheral phenyl rings, perpendicular to the macrocycle in D_{4h} and ruffled in S_4. As may be seen in Table VIII, the deviation from perpendicularity has only a minor effect on the calculated properties. The energies differ by only 0.05 eV, and the lengths of

Downloaded 13 Jun 2011 to 129.123.124.169. Redistribution subject to AIP license or copyright; see http://jcp.aip.org/about/rights_and_permissions

TABLE I. Calculated bond lengths (Å) in MTPP and MP (in parentheses). Atom labels from Fig. 1. Experimental data[a] reported for comparison.

		FeTPP	CoTPP	NiTPP	CuTPP	ZnTPP
R_{N-Ni}	Calc	1.970(1.975)	1.967(1.980)	1.968(1.969)	2.027(2.029)	2.060(2.062)
	Expt	1.972	1.949	1.957	1.981	2.042
R_{NI-C2}	Calc	1.396(1.390)	1.393(1.382)	1.389(1.382)	1.397(1.374)	1.379(1.372)
	Expt	1.382	1.383	1.396	1.385	1.374
R_{C1-C2}	Calc	1.393(1.384)	1.392(1.383)	1.391(1.380)	1.402(1.391)	1.410(1.399)
	Expt	1.392	1.384	1.398	1.369	1.409
R_{C2-C3}	Calc	1.435(1.436)	1.437(1.441)	1.440(1.440)	1.445(1.445)	1.447(1.447)
	Expt	1.436	1.435	1.427	1.449	1.425
$R_{C3-C3'}$	Calc	1.364(1.366)	1.362(1.362)	1.360(1.361)	1.363(1.365)	1.366(1.367)
	Expt	1.353	1.346	1.335	1.337	1.374

[a]X-ray diffraction data: FeTPP, Ref. 44; CoTPP, Ref. 45; NiTPP, Ref. 46 (in nickel etioporphyrin); CuTPP, Ref. 46; ZnTPP, Ref. 46 [in ZnTPP·$(H_2O)_2$]; the experimental values are averaged to give D_{4h} symmetry.

the Ni–N bond by only 0.02 Å. Ionization potentials are scarcely affected at all, as is the electron affinity of this species. Indeed, our finding of only minor perturbations confirms prior calculations. The ruffling of H_2TPP was found by AM1 and PM3 to change its ionization potentials by less than 0.1 eV.[42] The distortion of the D_{4h} geometry of NiTPP to S_4 was calculated by DFT-SQM to lower its energy by 0.07 eV,[43] in good agreement with our own value of 0.05 eV. In view of the small twists from D_{4h} symmetry, combined with their minimal effects upon the calculated properties, the various MTPPs were optimized under this geometrical restriction.

The optimized bond lengths for the various MPs and MTPPs are collected in Table I, together with their experimental correlates. For these large systems, there are only x-ray crystal diffraction data available.[44–46] Since the crystals exhibit small deviations from D_{4h}, the reported experimental values are averaged to D_{4h} symmetry.

The calculated M–N bond distances in FeTPP, CoTPP, and NiTPP are all close to 1.97 Å, notably shorter than in CuTPP and ZnTPP, which are around 2.05 Å. The bond between the N and the C of the imidazole ring shows similar clustering, with the Fe, Co, and Ni derivatives about 0.01 Å longer than for Cu and Zn. However, the remainder of the molecular geometry is little affected by the nature of the metal. Elimination of the four phenyl groups in TPP has little effect upon the geometry, as witnessed by the similarity of the values in parentheses in Table I. The agreement between the calculated and the available experimental data is quite good, particularly when considering the potential perturbations that might arise from crystal forces; the largest deviation is 0.05 Å for bond length and 1.5° for bond angle.

B. Electronic structures of MTPP and its ions

The computed energies of some of the higher occupied and lower unoccupied molecular orbitals (MOs) for the ground state of the five MTPP molecules are diagrammed in Fig. 2. Under D_{4h} symmetry, the five metal *3d*-orbitals transform as $a_{1g}(d_{z^2})$, $b_{1g}(d_{x^2-y^2})$, e_g (d_π, i.e., d_{xz} and d_{yz}), and $b_{2g}(d_{xy})$. The populations of some of the metal MOs are reported in parentheses so as to assist in interpretation. The relative energies of a variety of states of FeTPP, CoTPP, and a number of related ions are displayed in Table II. The calculated energy gaps between the highest occupied molecular orbital (HOMO) and lowest unoccupied molecular orbital (LUMO) in the MTPPs and their ions are listed in Table III.

Before describing the structures of the individual systems, there are a number of important patterns to note in Fig. 2. The HOMO and LUMO of the uncomplexed TPP are a_{1u} and a_{2u}, respectively. Both of these orbitals are stabilized by the addition of the metals, as in the b_{2u} orbital, but the energies of these porphyrin MOs are rather insensitive to the nature of the particular metal. As one moves across the periodic table from Fe to Zn, the energies of the metal *d*-orbitals tend to drop. This pattern is most evident and dramatic in the $d_{x^2-y^2}$ orbital. Note also that as the energy of this orbital falls into the range of the porphyrin MOs, the fractional contribution of the metal to the b_{1g} orbital diminishes, as a result of mixing. A similar trend of progressive stabilization is apparent for the $1e_g d_\pi$ and $b_{2g}d_{xy}$ levels. This mixing can result also in deviations from the general trend, causing, for instance, a jump in the d_{z^2} energy from CoTPP to NiTPP.

1. FeTPP

The lowest energy electronic configuration of FeTPP (and FeP) corresponds to $[\ldots](b_{2g})^2(a_{1g})^2(1e_g)^2, a\ ^3A_{2g}$ state, in agreement with the recent nonlocal DFT calculations of FeP by Kozlowski *et al.*[20] This is in agreement with the experimental assignment,[44,47–50] but differs from the previous DFT (DMol) calculations[15,18] that assign a ground state of ^3E_g to FeP. (Note from Table II that the ordering of the states in FeTPP is the same as that in FeP.) Our data indicate that ^3E_g is the second lowest state, 0.12 eV higher in energy. Mössbauer studies of FeTPP lead to a separation of 1.35 $\times$435 cm^{-1} (0.07 eV) between the $^3A_{2g}$ and ^3E_g states,[48] agreeing very well with the calculated value. Because ^3E_g and $^3A_{2g}$ are so close in energy, they may be mixed by spin–orbit coupling.[48,49] The third lowest state, $^3B_{2g}$, is some 0.3 eV above the ground state. Boyd *et al.*[49] used magnetic susceptibility measurements, together with ligand field calculations, to conclude that the ground state is ^3A_g followed by ^3E_g and $^3B_{2g}$ (in ascending order of energy), consistent with our calculations. The quintet state $^5A_{1g}$ lies 0.75 eV above $^3A_{2g}$, in comparison with a magnetic susceptibility measure-

Downloaded 13 Jun 2011 to 129.123.124.169. Redistribution subject to AIP license or copyright; see http://jcp.aip.org/about/rights_and_permissions

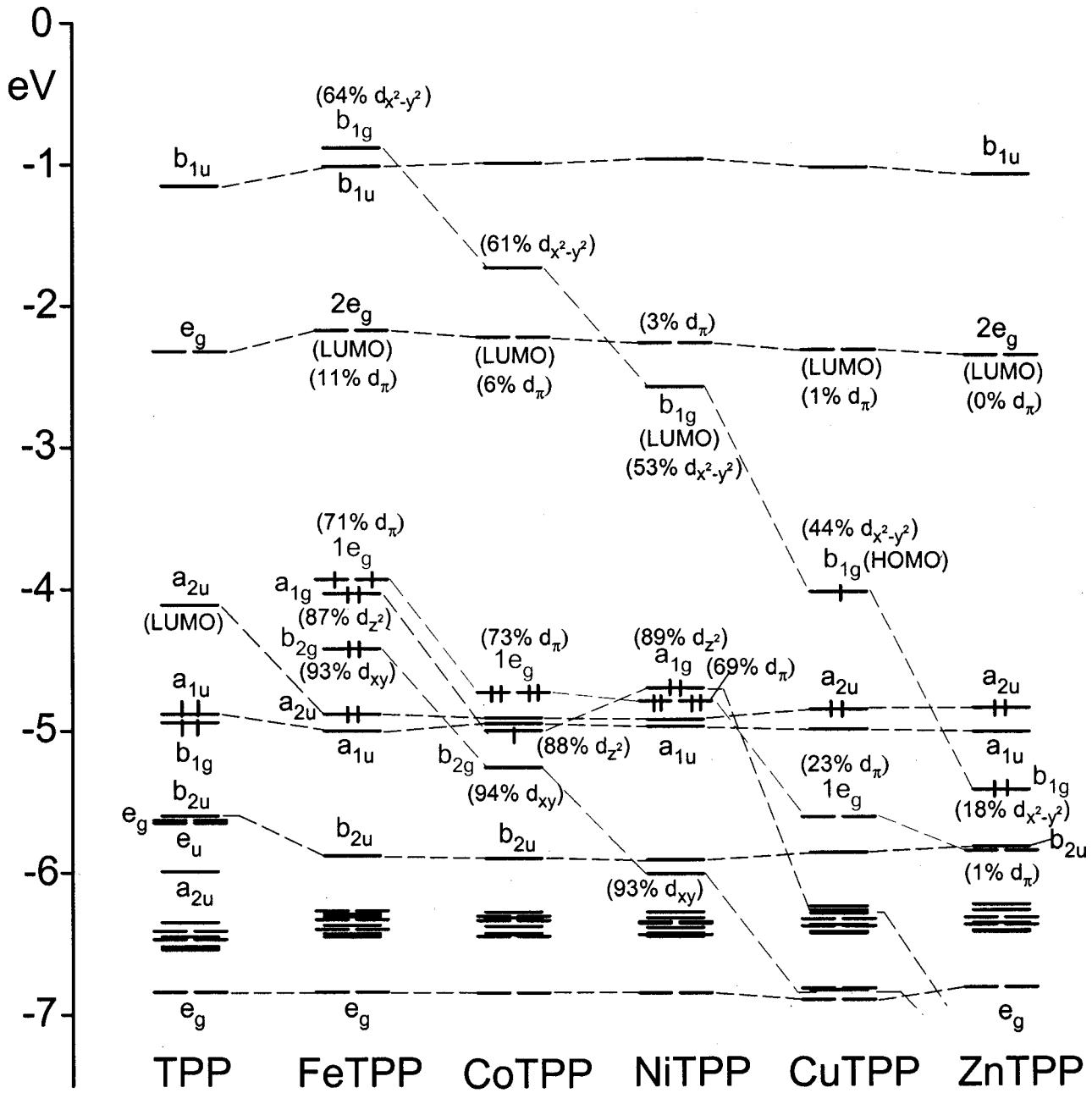

FIG. 2. Orbital energy levels for the outer orbitals of TPP (on left, with no H atoms in the porphyrin cage), and MTPPs. Metal $3d$ AO contributions of some MOs are listed in parentheses. Electron occupancies are indicated for frontier MOs.

ment that yielded a value of 5000 cm^{-1} (0.62 eV).[49] The lowest closed-shell state, $^1A_{1g}$, lies 1.5 eV above the ground state.

Perusal of the second column of Fig. 2 shows that the four occupied $3d$-like orbitals $b_{2g}(d_{xy})$, $a_{1g}(d_{z^2})$, and $1e_g(d_\pi)$, all lie above the porphyrin a_{2u} orbital. The d_{z^2} and d_π orbitals are weakly antibonding; higher in energy than the nonbonding d_{xy}. The unoccupied $b_{1g}(d_{x^2-y^2})$ is strongly antibonding, lying above the empty porphyrin b_{1u}. The a_{2u} and $2e_g(\pi^*)$ are the HOMO and LUMO, respectively, of the porphyrin ring in FeTPP. The latter orbital contains a contribution of about 10% from the metal. The occupied a_{2u} and a_{1u} from the porphyrin are almost degenerate and well separated from lower-lying levels, a feature of free-based porphyrins (H_2P).[51] There is little influence of the metal on the porphyrin a_{1u} energy level, indicating that the interaction between the metal π and the porphyrin π orbitals is minimal. Examination of the orbital levels in the smaller FeP reveals that the outer MOs are quite similar to those of FeTPP. The major difference is that the MO diagram of MP does not contain the phenyl orbitals which form a band at relatively low energy.

Examination of Fig. 3 illustrates the behavior of the various orbital energies as electrons are removed from (left) or added to (right) the FeTPP species. The effect of reduction is fairly simple in that the orbitals all move upward in energy. The amount of this upward translation is not quite uniform from one to the next, resulting in some switching of the metal d-orbitals in going from FeTPP to $[FeTPP]^{2-}$. The oxidation patterns are more complex in that while all orbitals

Downloaded 13 Jun 2011 to 129.123.124.169. Redistribution subject to AIP license or copyright; see http://jcp.aip.org/about/rights_and_permissions

TABLE II. Calculated relative energies (eV) for selected configurations of MTPP and MP (in parentheses).

	Configuration	Term	E^{rel}	Oxidation or reduction product
FeTPP	$(a_1u)^2(a_{2u})^2(b_{2g})^2(a_{1g})^2(1e_g)^2$	$^3A_{2g}$	0 (0)	
	$(a_1u)^2(a_{2u})^2(b_{2g})^2(a_{1g})^1(1e_g)^3$	$^3E_g(A)$	0.12 (0.12)	
	$(a_1u)^2(a_{2u})^2(b_{2g})^2(a_{1g})^1(1e_g)^4$	$^3B_{2g}$	0.28 (0.26)	
	$(a_1u)^2(a_{2u})^2(b_{2g})^2(a_{1g})^2(1e_g)^3$	$^3E_g(B)$	0.72 (0.74)	
	$(a_{1u})^2(a_{2u})^2(b_{2g})^1(a_{1g})^2(1e_g)^2(b_{1g})^1$	$^5A_{1g}$	0.75 (0.71)	
	$(a_{1u})^2(a_{2u})^2(b_{2g})^2(a_{1g})^1(1e_g)^2(b_{1g})^1$	$^5B_{2g}$	1.09 (1.05)	
	$(a_{1u})^2(a_{2u})^2(b_{2g})^2(a_{1g})^0(1e_g)^4$	$^1A_{1g}$	1.15 (1.49)	
$[FeTPP]^+$	$(a_{1u})^2(a_{2u})^2(b_{2g})^2(a_{1g})^1(1e_g)^2$	$^4A_{1g}$	0 (0)	$[Fe^{III}TPP]^+$
	$(a_{1u})^2(a_{2u})^2(b_{2g})^1(a_{1g})^2(1e_g)^2$	$^4B_{1g}$	0.33 (0.34)	
	$(a_{1u})^2(a_{2u})^1(b_{2g})^2(a_{1g})^2(1e_g)^2$	$^4A_{1u}$	0.58 (0.71)	
	$(a_{1u})^1(a_{2u})^2(b_{2g})^2(a_{1g})^2(1e_g)^2$	$^4A_{2u}$	0.68 (0.71)	
	$(a_{1u})^2(a_{2u})^2(b_{2g})^2(a_{1g})^2(1e_g)^1$	^2E_g	0.94 (0.97)	
$[FeTPP]^-$	$(b_{2g})^2(a_{1g})^1(1e_g)^4$	$^2A_{1g}$	0 (0)	$[Fe^{I}TPP]^-$
	$(b_{2g})^2(a_{1g})^2(1e_g)^3$	^2E_g	0.25 (0.26)	
	$(b_{2g})^2(a_{1g})^2(1e_g)^2(2e_g)^1$	^4E_g	0.56	
$[FeTPP]^{3-}$	$(b_{2g})^2(1e_g)^4(a_{1g})^2(2e_g)^1$	^2E_g	0	$[Fe^0TPP]^{3-}$
	$(b_{2g})^2(1e_g)^4(a_{1g})^1(2e_g)^2$	$^4A_{2g}$	0.05	
CoTPP	$(a_{1u})^2(a_{2u})^2(a_{1g})^1(1e_g)^4$	$^2A_{1g}$	0 (0)	
	$(a_{1u})^2(a_{2u})^2(a_{1g})^2(1e_g)^3$	^2E_g	0.22 (0.26)	
$[CoTPP]^+$	$(a_{1u})^2(a_{2u})^2(a_{1g})^2(1e_g)^2$	$^3A_{2g}$	0 (0)	$[Co^{III}TPP]^+$
	$(a_{1u})^2(a_{2u})^1(a_{1g})^1(1e_g)^4$	$^3A_{2u}$	0.23 (0.26)	
	$(a_{1u})^1(a_{2u})^2(a_{1g})^1(1e_g)^4$	$^3A_{1u}$	0.30 (0.28)	
	$(a_{1u})^2(a_{2u})^2(a_{1g})^1(1e_g)^3$	^3E_g	0.38 (0.36)	
$[CoTPP]^{2+}$	$(a_{1u})^1(a_{2u})^2(a_{1g})^2(1e_g)^2$	$^4A_{2u}$	0	$[Co^{III}TPP]^{2+}$
	$(a_{1u})^2(a_{2u})^1(a_{1g})^2(1e_g)^2$	$^4A_{1u}$	0.03	
$[CoTPP]^{4-}$	$(1e_g)^4(a_{1g})^2(2e_g)^2(b_{1g})^1$	$^4B_{2g}$	0	$[Co^0TPP]^{4-}$
	$(1e_g)^4(a_{1g})^2(2e_g)^3(b_{1g})^0$	^2E_g	0.48	
NiTPP	$(a_{1u})^2(a_{2u})^2(1e_g)^4(a_{1g})^2$	$^1A_{1g}$		
$[NiTPP]^+$	$(a_{1u})^2(a_{2u})^1(1e_g)^4(a_{1g})^2$	$^2A_{2u}$	0 (0)	$[Ni^{II}TPP]^+$
	$(a_{1u})^1(a_{2u})^2(1e_g)^4(a_{1g})^2$	$^2A_{1u}$	0.07 (0.03)	
	$(a_{1u})^2(a_{2u})^2(1e_g)^3(a_{1g})^2$	^2E_g	0.33 (0.25)	
	$(a_{1u})^2(a_{2u})^2(1e_g)^4(a_{1g})^1$	$^2A_{1g}$	0.86	
$[NiTPP]^{2+}$	$(a_{2u})^1(a_{1u})^1(1e_g)^4(a_{1g})^2$	$^3A_{2g}$	0	$[Ni^{II}TPP]^{2+}$
	$(a_{2u})^1(a_{1u})^2(1e_g)^3(a_{1g})^2$	^3E_g	0.19	
	$(a_{2u})^1(a_{1u})^2(1e_g)^4(a_{1g})^1$	$^3A_{2u}$	0.81	
$[NiTPP]^-$	$(1e_g)^4(a_{1g})^2(2e_g)^1(b_{1g})^0$	^2E_g	0 (0)	$[Ni^{II}TPP]^-$
	$(1e_g)^4(a_{1g})^2(2e_g)^0(b_{1g})^1$	$^2B_{1g}$	0.08 (0.02)	
$[NiTPP]^{2-}$	$(1e_g)^4(a_{1g})^2(2e_g)^2(b_{1g})^0$	$^3A_{2g}$	0 (0)	$[Ni^{II}TPP]^{2-}$
	$(1e_g)^4(a_{1g})^2(2e_g)^1(b_{1g})^1$	^3E_g	0.21 (0.10)	
$[NiTPP]^{3-}$	$(1e_g)^4(a_{1g})^2(2e_g)^3(b_{1g})^0$	^2E_g	0 (0.17)	$[Ni^{II}TPP]^{3-}$
	$(1e_g)^4)(a_{1g})^2(2e_g)^2(b_{1g})^1$	$^4B_{2g}$	0.08 (0)	
$[NiTPP]^{4-}$	$(1e_g)^4(a_{1g})^2(2e_g)^3(b_{1g})^1$	^3E_g	0 (0.85)	$[Ni^{I}TPP]^{4-}$
	$(1e_g)^4(a_{1g})^2(2e_g)^2(b_{1g})^2$	$^3A_{2g}$	0.10 (0)	
	$(1e_g)^4(a_{1g})^2(2e_g)^4(b_{1g})^0$	$^1A_{1g}$	0.28 (1.98)	
CuTPP	$(a_{1u})^2(a_{2u})^2(b_{1g})^1$	$^2B_{1g}$		
$[CuTPP]^+$	$(a_{2u})^1(a_{1u})^2(b_{1g})^1$	$^3B_{2u}$	0 (0)	$[Cu^{II}TPP]^+$
	$(a_{2u})^2(a_{1u})^1(b_{1g})^1$	$^3B_{1u}$	0.16 (0.07)	
	$(a_{2u})^2(a_{1u})^2(b_{1g})^0$	$^1A_{1g}$	0.38 (0.27)	
$[CuTPP]^{2+}$	$(a_{2u})^1(a_{1u})^1(b_{1g})^1$	$^3B_{2g}$	0	$[Cu^{II}TPP]^{2+}$
	$(a_{2u})^1(a_{1u})^2(b_{1g})^0$	$^2A_{2u}$	0.28	
$[CuTPP]^-$	$(a_{1u})^2(a_{2u})^2(b_{1g})^1(2e_g)^1$	^3E_g	0 (0)	$[Cu^{II}TPP]^-$
	$(a_{1u})^2(a_{2u})^2(b_{1g})^2(2e_g)^0$	$^1A_{1g}$	0.24 (0.15)	
$[CuTPP]^{2-}$	$(a_{1u})^2(a_{2u})^2(b_{1g})^1(2e_g)^2$	$^4B_{2g}$	0 (0)	$[Cu^{II}TPP]^{2-}$
	$(a_{1u})^2(a_{2u})^2(b_{1g})^2(2e_g)^1$	^2E_g	0.25 (0.24)	
$[CuTPP]^{3-}$	$(a_{1u})^2(a_{2u})^2(b_{1g})^1(2e_g)^3$	^3E_g	0 (0.23)	$[Cu^{II}TPP]^{3-}$
	$(a_{1u})^2(a_{2u})^2(b_{1g})^2(2e_g)^2$	$^3A_{2g}$	0.02 (0)	
$[CuTPP]^{4-}$	$(a_{1u})^2(a_{2u})^2(b_{1g})^2(2e_g)^3$	^2E_g	0 (0)	$[Cu^{I}TPP]^{4-}$
	$(a_{1u})^2(a_{2u})^2(b_{1g})^1(2e_g)^4$	$^2B_{1g}$	0.26 (0.91)	
$[ZnTPP]^+$	$(a_{1u})^2(a_{2u})^1$	$^2A_{2u}$	0	$[Zn^{II}TPP]^+$
	$(a_{1u})^1(a_{2u})^2$	$^2A_{1u}$	0.17	

Downloaded 13 Jun 2011 to 129.123.124.169. Redistribution subject to AIP license or copyright; see http://jcp.aip.org/about/rights_and_permissions

TABLE III. Calculated energy gaps (eV) between the LUMO and HOMO in MTPP (and MP) and related ions.

	M=Fe	M=Co	M=Ni	M=Cu	M=Zn
$[MTPP]^{2+}$	2.14	2.43	2.04	1.85	2.57
$[MTPP]^{1+}$	2.64(2.77)	2.42(2.42)	2.08(2.03)	1.82(1.82)	2.59(2.66)
MTPP	1.86(1.87)	2.50(2.55)	2.13(2.10)	1.71(1.75)	2.49(2.60)
$[MTPP]^{1-}$	1.58(1.65)	1.30(1.31)	0.35(0.53)	1.42(1.75)	1.47(1.74)
$[MTPP]^{2-}$	0.88(1.17)	0.78(1.47)	0.48(0.38)	1.06(1.68)	1.08(1.68)
$[MTPP]^{3-}$	0.59(0.98)	0.68(1.16)	0.54(0.86)	0.93(1.03)	0.94(1.62)
$[MTPP]^{4-}$	0.35(0.08)	0.86(1.04)	0.85(1.40)	1.01(1.48)	0.89(1.55)

are stabilized by extraction of the first electron, the occupied MOs move upward in energy when the second electron is removed. Since the magnitudes of these energy changes are highly variable, there is a good deal of orbital switching associated with mono- and dioxidation.

As indicated in Table II, the ground state of cationic $[FeTPP]^+$ corresponds to $^4A_{2g}[(b_{2g})^2(a_{1g})^1(1e_g)^2]$. Thus the first oxidation takes place from the central metal (d_{z^2}), in accord with electron spin resonance (ESR) measurements.[25] It is noteworthy that the singly occupied a_{1g} is situated below a number of doubly occupied orbitals in the monocation. A second oxidation of $[FeTPP]^+$ to yield $[FeTPP]^{2+}$ occurs from the a_{2u} orbital (see Fig. 3), i.e., the porphyrin ring, leaving this ion with four unpaired electrons. This is again in agreement with ESR measurements.[25] The first and second reductions of FeTPP to yield $[FeTPP]^-$ and $[FeTPP]^{2-}$ involves electron addition to the low-lying half-filled metal *d*-orbitals. $[FeTPP]^-$ has a ground state of $^2A_{1g}[(b_{2g})^2(a_{1g})^1(1e_g)^4]$ wherein the added electron goes into $1e_g$, along with some rearrangement of the *d*-electrons. For the third and fourth reductions, electrons enter the LUMO $2e_g$ on the porphyrin ring, as the metal a_{1g} is completely filled.

2. CoTPP

For the low-spin $(S=1/2)$ CoTPP,[52] the ground state configuration is known to be $(d_{xy})^2(d_\pi)^4(d_{z^2})^1$ from analysis of the ESR spectra.[53] Our calculation is consistent with this assignment. Although the a_{1g} orbital lies below $1e_g$ (see Fig. 2), the ground state is nevertheless $^2A_{1g}$ from configuration $(a_{1g})^1(1e_g)^4$, leaving the $1e_g$ HOMO fully occupied. This effect may be due to the favorable electrostatic energy of the electrons offsetting the less favorable ligand field energy. On the other hand, the ^2E_g state arising from configuration $(a_{1g})^2(1e_g)^3$ lies only 0.2 eV higher in energy than the $^2A_{1g}$ ground state. The a_{2u} and a_{1u} orbitals of the porphyrin lie between the two latter orbitals, and represent HOMO-1 and HOMO-2, respectively. Unlike FeTPP, the unoccupied $b_{1g}(d_{x^2-y^2})$ is lower than b_{1u}, but still lies above the $2e_g$ LUMO. Again compared to FeTPP, the LUMO in CoTPP contains less contribution from $M-d_\pi$.

The $[CoTPP]^+$ ion has a $^3A_{2g}$ ground state, quite similar to the isoelectronic neutral FeTPP. According to the calculation, the first ionization potential of $[CoTPP]^+$ corresponds to the removal of an electron from the porphyrin a_{2u} orbital, leaving the higher-energy $1e_g$ orbitals occupied (see Sec.

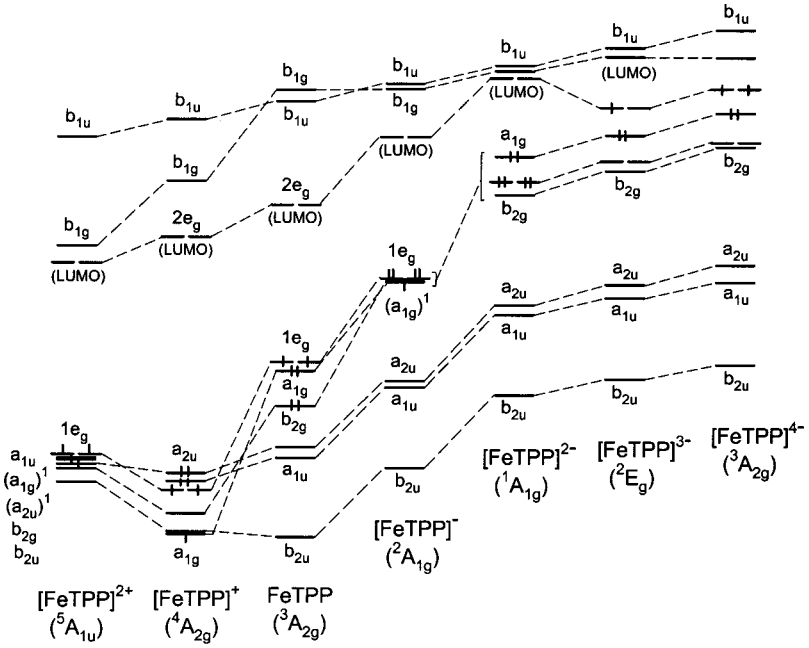

FIG. 3. Orbital energy levels of [FeTPP] and its ions in the HOMO–LUMO region.

Downloaded 13 Jun 2011 to 129.123.124.169. Redistribution subject to AIP license or copyright; see http://jcp.aip.org/about/rights_and_permissions

III C for more details). Therefore the initial oxidation of CoTPP involves the abstraction of an electron from the porphyrin ring to yield a $[Co^{II}TPP]^+$ radical. Then an internal redistribution of electrons takes place, i.e., an electron transfers from metal to ring: $Co^{II} \rightarrow Co^{III}$. A further oxidation to $[CoTPP]^{2+}$ occurs from the porphyrin a_{1u}, but there is a near degeneracy of $^4A_{2u}$ with $^4A_{1u}$, which results from electron abstraction from a_{2u}.

In the case of reduction, the MO energy diagram of CoTPP suggests that the added electron ought to be placed in the low half-filled $a_{1g}(d_{z^2})$ level. Indeed, electron uptake by a metal-centered orbital has been evidenced by a polarographic study of CoTPP.[54] X-ray photoelectron spectroscopy (XPS) results are consistent, revealing the formation of Co^I species.[27] The second and third reductions involve electron addition to the porphyrin $2e_g$. On the fourth reduction, however, an added electron is accommodated in the metal $b_{1g}(d_{x^2-y^2})$, resulting in the formation of Co^0.

3. NiTPP

The Ni porphyrin is calculated to be diamagnetic (closed shell), in agreement with experimental observation.[55] In contrast to the Fe and Co cases, the $a_{1g}(d_{z^2})$ orbital rises above $1e_g(d_\pi)$ to become the HOMO. The $b_{1g}(d_{x^2-y^2})$ orbital is located well above the HOMO (a_{1g}) but lower than $2e_g$, making it the LUMO. The b_{2g} orbital retains its heavy d_{xy} participation and continues its drop in energy.

In contrast to an earlier suggestion that the first oxidation of NiTPP occurs at the central metal,[25] the calculations indicate instead that it is a porphyrin a_{2u} (or a_{1u}) orbital from which the electron is removed, and not from the higher-lying metal a_{1g} (HOMO) or $1e_g$ (HOMO-1) orbitals. $[Ni^{III}TPP]^+$ was found to be unstable and gradually decayed via internal electron transfer to a $[Ni^{II}TPP]^+$ cation radical,[24] in accord with our calculations which find the former to be 0.33 eV less stable than the latter. The second oxidation occurs from the other porphyrin (a_{1u}) orbital. In the case of reduction, the first three electrons are added to the porphyrin $2e_g(\pi^*)$ orbitals, leaving $b_{1g}(d_{x^2-y^2})$ unoccupied, since addition of electrons to $2e_g$ raises the energy of b_{1g}, placing the latter above the former. However, the fourth reduction takes place into the metal $b_{1g}(d_{x^2-y^2})$.

The smaller model system NiP obeys much the same trends for the first two added electrons. However, in the case of the third reduction, the electron goes not to the porphyrin but rather to the metal, and in $[NiP]^{4-}$ the b_{1g} is fully occupied.

4. CuTPP

The $3d$-orbitals of Cu are low in energy and the odd electron occupies the $b_{1g}(d_{x^2-y^2})$ HOMO. As evident in Table II, the first oxidation occurs from $a_{2u}(^3B_{2u})$ although the HOMO lies some 0.8 eV higher. Our calculation agrees with the ESR measurements,[1] but differs from the prior MS-Xα calculation,[13] which indicates that the first electron is removed from the porphyrin a_{1u} orbital. Oxidation from a_{1u}, which gives a $^3B_{1u}$ state, requires 0.2 eV more than that from a_{2u}. For the model CuP system, the energy gap between $^3B_{2u}$ and $^3B_{1u}$ is reduced to 0.07 eV, so it may be that peripheral substituents are necessary to distinguish between these two states. The second oxidation is calculated to occur at the porphyrin (a_{1u}), again in agreement with experiment.[1,25]

Based upon the MO energy diagram of CuTPP in Fig. 2, one might expect an added electron to go into the $b_{1g}(d_{x^2-y^2})$ orbital, a d^{10} configuration. However, the calculation assigns this additional electron to $2e_g(d^9)$ by 0.24 eV, consonant with polarographic studies.[54] Our calculation thus does not support the XPS[27] and MS-Xα calculated[13] results which favor d^{10}. Our preference for $2e_g$ may be due to the relatively large $d-d$ repulsion energy involved in pairing b_{1g} electrons. The second reduction step corresponds to addition to $2e_g$ as well. The third reduction may involve either b_{1g} or $2e_g$ because the ^3E_g and $^3A_{2g}$ states are almost degenerate. (For the model system CuP, the third electron is clearly added to the b_{1g}.) On a fourth reduction, the electron enters b_{1g}.

5. ZnTPP

The $3d$-orbitals are particularly low in energy for Zn. Indeed, contrary to the other molecules, the HOMO in ZnTPP is no longer a M$-3d$ orbital. The b_{1g} has lost all but 18% of its M contribution, and is largely porphyrin σ in character. The first oxidation of ZnTPP leads to a π-cation radical, where the electron is removed from the HOMO a_{2u}, leading to a $^2A_{2u}$ ground state. This is in accord with ESR.[56] The second oxidation gives a π-dication with a $^3A_{2g}$ state. In the reduction stages, four electrons are accommodated in the LUMO $2e_g(\pi^*)$, again in agreement with experiment.[23] In the $[ZnTPP]^{x-}$ anions, there is no $3d$-like orbital near $2e_g$, different from the other $[MTPP]^{x-}$ species.

6. HOMO–LUMO gaps

The difference in energy between the HOMO and LUMO of each of the various TPP complexes is reported in Table III. As one goes across the periodic table from Fe to Zn, there is a fluctuating trend in these energy gaps for the neutrals. The gap increases from Fe to Co, then decreases through Ni and Cu, before rising again in the case of Zn. The addition of electrons gradually leads to a progressive reduction in the energy gap, although there are discrepancies, e.g., $[MTPP]^{3-}$ to $[MTPP]^{4-}$ for Co, Ni, and Cu. Removal of electrons yields erratic trends in the HOMO–LUMO gaps, in some cases not much of a change from the neutral. It might be noted lastly that the change from TPP to the simpler P produces large changes in the energy gap in a number of cases, particularly for the highly charged anions.

7. Mulliken population analysis

The calculated gross populations of selected atomic orbitals and Mulliken atomic charges (Q_M) are collected in Table IV. The ''effective'' charge of each metal atom, corresponding to the fourth row of Table IV, lies in the range of $+0.5\pm0.1$ for the neutral molecules, quite different from the classical picture of $M^{2+}(TPP)^{2-}$, wherein two $4s$ electrons have been lost by the metal. This discrepancy may be ratio-

Downloaded 13 Jun 2011 to 129.123.124.169. Redistribution subject to AIP license or copyright; see http://jcp.aip.org/about/rights_and_permissions

TABLE IV. Gross Mulliken populations and atomic charges (Q) in MTPPs and their ions, and MP analogs (in parentheses).

		M=Fe	M=Co	M=Ni	M=Cu	M=Zn
MTPP	$3d$	6.58(6.57)	7.60(7.60)	8.62(8.61)	9.52(9.51)	10.0(10.0)
	$4s$	0.46(0.44)	0.36(0.34)	0.45(0.43)	0.42(0.41)	0.59(0.58)
	$4p$	0.33(0.33)	0.47(0.47)	0.52(0.51)	0.52(0.52)	0.80(0.79)
	Q_M	0.63(0.66)	0.57(0.59)	0.42(0.44)	0.55(0.57)	0.61(0.63)
	Q_N	−0.49(−0.47)	−0.46(−0.43)	−0.44(−0.42)	−0.45(−0.43)	−0.45(−0.43)
	Q_{C1}	−0.02(0.10)	−0.02(0.10)	−0.02(0.10)	−0.03(0.09)	−0.03(0.08)
	Q_{C2}	0.28(0.26)	0.28(0.26)	0.28(0.27)	0.27(0.26)	0.27(0.26)
$[MTPP]^+$	$3d$	6.50(6.49)	7.53(7.52)	8.63(8.61)	9.52(9.52)	10.0(10.0)
	$4s$	0.33(0.31)	0.40(0.38)	0.43(0.41)	0.40(0.39)	0.58(0.56)
	$4p$	0.41(0.40)	0.46(0.46)	0.50(0.50)	0.50(0.49)	0.78(0.77)
	Q_M	0.77(0.80)	0.60(0.63)	0.45(0.48)	0.58(0.60)	0.64(0.67)
$[MTPP]^{2+}$	$3d$	6.39	7.54	8.63	9.52	10.0
	$4s$	0.32	0.39	0.41	0.39	0.57
	$4p$	0.42	0.45	0.49	0.49	0.77
	Q_M	0.88	0.62	0.47	0.60	0.66
$[MTPP]^-$	$3d$	6.68(6.68)	7.72(7.72)	8.62(8.67)	9.52(9.51)	10.0(10.0)
	$4s$	0.37(0.35)	0.50(0.48)	0.47(0.47)	0.43(0.42)	0.60(0.59)
	$4p$	0.35(0.35)	0.39(0.39)	0.52(0.48)	0.53(0.53)	0.80(0.79)
	Q_M	0.60(0.62)	0.39(0.41)	0.39(0.38)	0.52(0.54)	0.60(0.61)
$[MTPP]^{2-}$	$3d$	6.69(6.69)	7.72(7.73)	8.63(8.62)	9.52(9.51)	10.0(10.0)
	$4s$	0.56(0.56)	0.53(0.53)	0.49(0.49)	0.44(0.44)	0.61(0.61)
	$4p$	0.31(0.30)	0.39(0.39)	0.52(0.52)	0.54(0.54)	0.81(0.80)
	Q_M	0.45(0.44)	0.36(0.35)	0.37(0.37)	0.51(0.51)	0.58(0.59)
$[MTPP]^{3-}$	Q_M	0.41(0.34)	0.32(0.27)	0.35(0.31)	0.49(0.41)	0.57(0.57)
$[MTPP]^{4-}$	Q_M	0.37(0.32)	0.29(0.35)	0.33(0.38)	0.48(0.45)	0.56(0.56)

nalized on the basis of σ/π bonding and charge transfer from $(TPP)^{2-}$ to M^{2+}. As one goes across the periodic table from Fe to Ni, this charge diminishes from 0.6 to 0.4, but then climbs again on going from Ni to Zn. The metal $4s$ population lies in the vicinity of 0.4–0.6 with no obvious pattern from one metal to the next. The $4p$ populations are of a similar magnitude and appear to climb on going across from Fe to Zn. The fractional occupation numbers of the $3d$-shells show the most dependence upon the nature of the metal, climbing from a minimum of 6.5 for Fe up to the full occupancy 10 of Zn. With the exception of the latter, there are about 0.6 additional electrons in the M-$3d$ orbitals, beyond the classical ligand field d^{n-2} configuration. This increase in the M-$3d$ populations can be ascribed to backdonation from the π orbitals of the porphyrin skeleton to the M-$3d$ atomic orbitals.

Turning to the porphyrin, the high electronegativity of nitrogen leads to some accumulation of charge. The net charge on N is −0.45 to −0.50 in the complexes with the metals, some 0.2–0.3 more negative than in the uncomplexed porphyrin. The C_1 atoms that bridge the imidazole rings are essentially neutral, and are little affected by complexation with the metal. The C_2 atoms, part of the imidazole rings, pick up a small amount of positive charge when the metal is added. The remainder of the porphyrin atoms are insensitive to complexation. It is further important to stress that the orbital populations and atomic charges are nearly identical for MTPP and its smaller model MP analogs.

Concerning the ions, removal of the electrons has only a small effect upon the charge of the metal, only 0.03 for the first electron, and 0.02 for the second. The atomic orbitals are similarly insensitive to the ionic nature of the complex. The exception is FeTPP where these increments in atomic charge are 0.14 and 0.11, respectively. The $3d$ orbitals of the Fe parallel these changes fairly closely while the $4p$ population increases upon going from 0 to +1. As in the case of the cations, the charge assigned to the metal in the anionic $[MTPP]^-$ is also quite similar to that in the neutral, except for M=Co, where the charge in $[CoTPP]^-$ is 0.2 less positive than in CoTPP. From the last rows of Table IV, it may be seen that further reductions add only small increments of atomic charges to the metal.

C. M–TPP binding energies, ionization potentials, and electron affinities

Table V displays the calculated values for M–TPP binding energies (E_{bind}), first and second ionization potentials (IP), and electron affinities (EA), together with any available experimental data.[57–63] These quantities are defined in terms of the energies of the various species as follows:

$$-E_{bind}=E(MTPP)-\{E(M)+E(TPP)\},$$

$$IP=E(MTPP^{(x+1)+})-E(MTPP^{x+}) \quad (x=0,1),$$

$$EA=E(MTPP^{(x+1)-})-E(MTPP^{x-}) \quad (x=0,1,2,3).$$

The calculated binding energy is 10.1 eV for FeTPP, rises to 10.8 eV for CoTPP, and then diminishes steadily until reaching a minimum of 6.3 eV for ZnTPP. The equivalent quantities for the model MP analogs are consistently larger by 0.2 eV, indicating that the peripheral phenyl rings act to reduce the binding of the metal by this small amount. These strong interactions between the metal and the porphyrin can be related to the high thermal and chemical stability of metal

Downloaded 13 Jun 2011 to 129.123.124.169. Redistribution subject to AIP license or copyright; see http://jcp.aip.org/about/rights_and_permissions

TABLE V. Calculated M–TPP binding energies in MTPP (E_{bind}), first and second ionization potentials of MTPP (IP), electron affinities of $[\text{MTPP}]^x$ (EA) ($x=0,1-,2-,3-$), and disproportionation reaction energies (eV) for reaction $2[\text{MTPP}]^{x-}\rightarrow[\text{MTPP}]^{(x-1)-}+[\text{MTPP}]^{(x+1)-}$. Values in parentheses refer to the model MP systems. All quantities in electron volts.

		M=Fe	M=Co	M=Ni	M=Cu	M=Zn
E_{bind}		10.07(10.25)	10.81(11.01)	9.94(10.13)	7.63(7.82)	6.32(6.52)
First IP	Calc	5.97(6.29)	6.57(6.98)	6.59(7.01)	6.51(6.96)	6.50(6.94)
	Expt[a]			6.44	6.49	6.42
Second IP		9.63(10.54)	9.65(10.57)	9.61(10.65)	9.62(10.64)	9.61(10.61)
EA ($x=0$)	Calc	−1.82(−1.66)	−2.13(−1.96)	−1.49(−1.31)	−1.57(−1.38)	−1.60(−1.40)
	Expt[b]	−1.87±0.03		−1.51±0.01		
($x=-1$)		1.59(2.22)	1.52(2.29)	1.34(2.14)	1.27(2.02)	1.24(1.99)
($x=-2$)		3.91(5.56)	4.02(5.63)	4.09(5.63)	3.82(5.46)	4.04(5.64)
($x=-3$)		6.48(8.95)	6.19(7.61)	6.20(7.26)	6.19(8.26)	6.43(8.88)
Disproportionation reaction energies						
$2[\text{MTPP}]^-\rightarrow\text{MTPP}+[\text{MTPP}]^{2-}$		3.66	3.65	2.83	2.84	2.84
$2[\text{MTPP}]^{2-}\rightarrow[\text{MTPP}]^-+[\text{MTPP}]^{3-}$		2.32	2.51	2.76	2.80	2.80
$2[\text{MTPP}]^{3-}\rightarrow[\text{MTPP}]^{3-}+[\text{MTPP}]^{4-}$		2.57	2.17	2.11	2.14	2.38

[a]Reference 57.
[b]Reference 63.

porphyrins. The M–TPP bond strength follows the same pattern derived from consideration of infrared spectral data.[59] The relatively weak Zn–TPP interaction is likely due to the absence of $3d$-orbital interactions, precluding π backdonation. The trend in the binding energies parallels the M–N bond lengths (see Table I) in that large E_{bind} is associated with shorter $R_{\text{M–N}}$.

The first calculated IP is 6.0 eV for FeTPP, and 6.5–6.6 eV for the various other MTPP species. Experimental gas-phase IPs have been reported for FeTPP, NiTPP, CuTPP, and ZnTPP.[57] Because the M-$3d$ electron bands are hard to detect,[60] the UV PE spectra[57] mainly show the porphyrin π bands, and therefore the first (lowest) detectable IP spectral bands arise from orbitals of the porphyrin π system without metal contribution. According to the calculation, the electron is first removed from a $3d$-like orbital for FeTPP, while it is in fact removed from the porphyrin π system for the other MTPPs. It is thus understandable that the first IPs for CoTPP through ZnTPP are similar, and notably larger than that of FeTPP. Both calculation and experiments[57,58] show that the IPs from porphyrin orbitals are insensitive to the nature of metal. Moreover, the calculated IPs are in quantitative agreement with the gas-phase PES values,[57] the error being less than 0.15 eV.

There seems to be no qualitative relation or correlation between the first IPs and the electrochemical oxidation potentials ($E_{1/2}$) of the porphyrin ring which exhibit substantial dependence upon the central metal.[28] The a_{1u} orbital in NiTPP has a higher IP than does a_{2u}, but the reverse situation is found for the other species. Another notable finding is that the ionized state of CoTPP$[^3A_{2u},(a_{2u})^1(a_{1g})^1(1e_g)^4]$ associated with the first ionization is different from the ground state of the cation $[^3A_{2g},(a_{2u})^2(a_{1g})^2(1e_g)^2]$, after electron transfer from metal to ligand has taken place. The IPs of MP are consistently 0.3–0.5 eV higher than those of MTPP, roughly consistent with the orbital energy shift. This trend is in agreement with experimental PES data for H_2P[61] and H_2TPP.[62] The second IP corresponds to electron ionization from the porphyrin a_{1u} (a_{2u} in the case of M=Ni) and is consequently independent of the metal. Four phenyl groups added to MP reduce the second IP by about 1 eV.

The calculated electron affinities (EAs) of MTPP are all quite negative, which indicates a strong attraction of an electron for each MTPP species. FeTPP and CoTPP are stronger in this regard than are the others. This observation can be understood on the basis of the electronic structures of the $[\text{MTPP}]^-$ ions. The added electron in $[\text{FeTPP}]^-$ and $[\text{CoTPP}]^-$ occupies a low-lying bonding orbital, whereas in the other $[\text{MPc}]^-$ ions, the added electron goes into a high-lying antibonding porphyrin $2e_g$. Experimental gas-phase EAs are available for FeTPP and NiTPP,[63] and are in excellent agreement with the calculations. The calculated EAs for MP are uniformly about 0.2 eV smaller. The progressively more positive entries for the anions in Table V are due to the increasing Coulomb repulsion between the ring charge and the added electrons.

Prior electrochemical measurements by Hush *et al.*[23] of the energies of disproportionation reactions $2[\text{MTPP}]^{x-}\rightarrow[\text{MTPP}]^{(x-1)-}+[\text{MTPP}]^{(x+1)-}(x=1,2,3)$ revealed that the disproportionation energies are positive and remarkably constant over a range of porphyrin structures, when M^{II} is a closed-shell system. The calculated energies of these reactions are reported in the last rows of Table V. They are all positive by more than 2 eV, and are of comparable magnitudes (2.8 eV) for M=Ni, Cu, and Zn, and for $x=1$ and 2, and diminish to the 2.1–2.4 eV range for $x=3$. The pattern for Fe and Co are different, owing to the different electronic structure of FeTPP/CoTPP, as compared to NiTPP/CuTPP/ZnTPP.

D. Effects of axial ligands

It is known that axial ligation has a substantial influence on the redox properties of metal porphyrins.[21,24,29] Six-coordinate iron porphyrins [e.g., FeTPP(pyridine)$_2$, FeTPP(piperidine)$_2$, FeTPP(pyridine)(CO)] are low-spin, diamagnetic ($S=0$) species.[24,44] While the ground state of four-coordinate cobalt porphyrins is somewhat ambiguous,[53]

Downloaded 13 Jun 2011 to 129.123.124.169. Redistribution subject to AIP license or copyright; see http://jcp.aip.org/about/rights_and_permissions

TABLE VI. Calculated properties of MTPP with two axial ligands L (L=Co, HCN).

		M=Fe	M=Co	M=Ni	M=Cu	M=Zn
E_{bind}[a] (eV)	L=Co	2.06	0.49	0.01	0.01	0.01
	L=HCN	1.00	0.12	0.01	0.01	0.01
R_{M-L} (Å)	L=CO	1.82	2.01	3.00	2.85	2.60
	Expt[b]	1.77				
	L=HCN	1.85	2.16	3.00	2.86	2.87
	Expt[c]	2.13	2.44			
R_{M-N} (Å)	L=CO	2.02	2.03	1.97	2.03	2.07
	Expt[b]	2.02				
	L=HCN	2.01	2.00	1.97	2.01	2.06
	Expt	2.00[c]	1.99[d]			
	No L	1.97	1.97	1.97	2.03	2.06
Q_M	L=CO	0.31	0.21	0.40	0.43	0.47
	L=HCN	0.50	0.47	0.50	0.56	0.65
	No L	0.63	0.57	0.42	0.55	0.61
Q_L	L=CO	0.10	0.12	0.04	0.07	0.09
	L=HCN	0.10	0.14	0.02	0.04	0.03
IP (eV)	L=CO	6.38(a_{2u},first)	5.81(a_{1g},first)			
			6.36(a_{2u})			
	L=HCN	6.05(a_{2u},first)	6.03(a_{2u},first)			
		6.21($1e_g$)	6.05(a_{1g})			
		6.30(b_{2g})				
	No L	5.97(a_{1g},first)	6.57(a_{2u},first)			
		6.55(a_{2u})	8.82(a_{1g})			
EA (eV)	L=CO	−1.56($2e_g$)	−1.58($2e_g$)			
			−0.84(a_{1g})			
	L=HCN	−1.20($2e_g$)	−1.16($2e_g$)			
			−0.32(a_{1g})			
	No L	−1.82($1e_g$)	−2.13(a_{1g})			
		−1.51($2e_g$)	−1.47($2e_g$)			

[a]Binding energy between MTPP and two L's.
[b]In crystal FeTPP(pyridine)CO complex (Ref. 65).
[c]In crystal FeTPP(piperidine)$_2$ complex (Ref. 67).
[d]In crystal CoTPP(piperidine)$_2$ (Ref. 66).

it appears certain that the ground state is $^2A_{1g}$ in solvent-coordinated complexes.[64] In a number of metal porphyrins, the site of oxidation/reduction is dependent on the nature of axial ligands.[24] These phenomena suggest that interaction with axial ligands may modify the electronic structure of metal porphyrins, motivating a systematic investigation of their effects on the electronic structure and other properties of the MTPPs. Two types of axial ligand were examined: CO is a strong π acceptor and HCN has strong σ-donor capacity but is a relatively weak π-bonder. These two molecules represent strong- and weak-field axial ligands, respectively. CO molecules were attached to the central metal with M–C–O in a linear arrangement, perpendicular to the porphyrin plane. This geometry has been observed in experiments with CO adsorbed on various metals. HCN was added in a similar geometry, with a linear M–N–C–H orientation, which was confirmed by geometry optimization. The calculated properties of MTPP(L)$_2$ (L=CO,HCN) are collected in Table VI and the changes of orbital levels in FeTPP and CoTPP are illustrated in Fig. 4.

1. L=CO

The binding energy between FeTPP and a pair of CO molecules is quite large, 2.1 eV. Much smaller but still appreciable at 0.5 eV is the same quantity for CoTPP–(CO)$_2$, whereas the binding energies of the other MTPPs listed in Table VI are nearly zero. The axial M–C distances, R(M–C$_{ax}$), correlate with the energetics to some degree, with R(Fe–C$_{ax}$) the shortest, followed by R(Co–C$_{ax}$). The calculated R(Fe–C$_{ax}$) of 1.82 Å compares favorably with the 1.77 Å measured in the FeTPP(pyridine)CO crystal.[65] The addition of two CO ligands to FeTPP expands the equatorial Fe–N bond distance, R(Fe–N$_{eq}$) by 0.05 Å compared with the unligated FeTPP, again in good agreement with the crystal structure data.[65] A similar M–N$_{eq}$ bond lengthening of 0.06 Å is found in CoTPP(CO)$_2$. In the other MTPP(CO)$_2$ complexes, the M–N$_{eq}$ distances are almost unchanged, again because of the extremely weak interaction between the two COs and the MTPP.

The perturbations caused in the MO energy diagram of MTPP are illustrated in Fig. 4 with the HCN ligand effects on the left, and the CO effects on the right. Perhaps the most striking feature of Fig. 4 is the very strong sensitivity of the energy of the a_{1g}(M-d_{z^2}) orbital in FeTPP and CoTPP to the presence of the ligands. This orbital is lifted by 2.6 and 2.2 eV in FeTPP(CO)$_2$ and CoTPP(CO)$_2$, respectively. The ligands also act to separate the a_{2u} and a_{1u} orbitals which are rather close in energy in their absence. Owing to the strong M→COπ* backbonding, the $1e_g$(M-d_π) orbitals are stabilized, placing them even lower than the porphyrin a_{1u} orbital. These reorderings result in a shift of electrons such that the HOMOs in FeTPP(CO)$_2$ and CoTPP(CO)$_2$ become, respectively, $(a_{2u})^2$ and $(a_{1g})^1$, yielding $^1A_{1g}$ and $^2A_{1g}$ ground states. (CoTPP has a $^2A_{1g}$ ground state, even in the absence of ligands).

The ligand-induced perturbation of the electronic struc-

Downloaded 13 Jun 2011 to 129.123.124.169. Redistribution subject to AIP license or copyright; see http://jcp.aip.org/about/rights_and_permissions

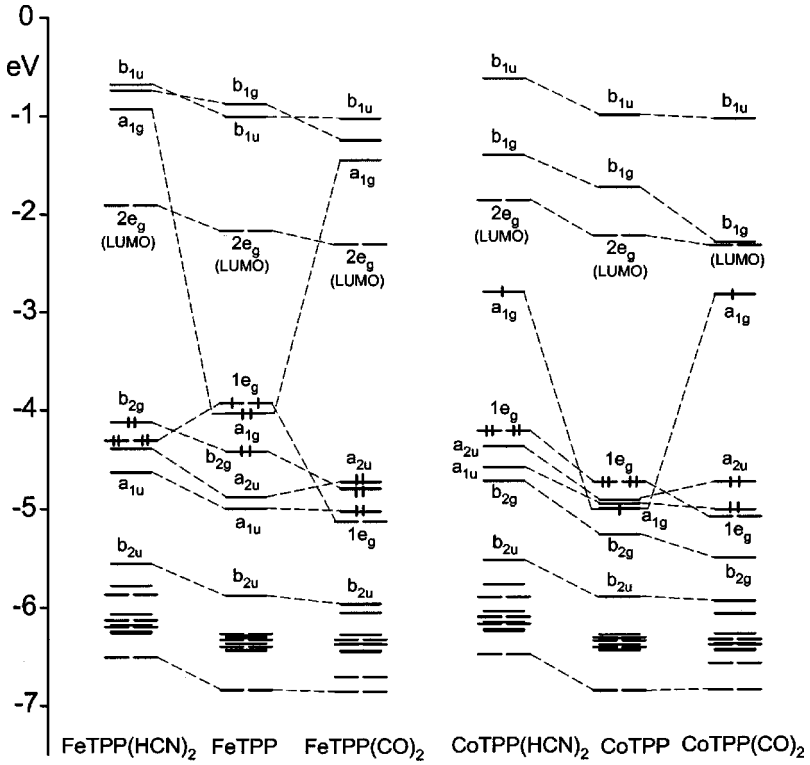

FIG. 4. Orbital energy levels of FeTPP (left) and CoTPP (right) when complexed with a pair of axial ligands (L=CO, HCN).

ture changes the calculated properties of the iron and cobalt porphyrins. In $FeTPP(CO)_2$, the first ionization now arises from the porphyrin a_{2u} (π) orbital and the following ionization occurs at the a_{1u}. This assignment is in agreement with electrochemical experiments[24] which showed a change in oxidation site upon axial coordination of RuTPP, a complex that is isoelectronic with FeTPP. The first IP value of $FeTPP(CO)_2$ is 0.4 eV higher than that of FeTPP (which is from the metal a_{1g}), while the CO ligands lower the a_{2u} IP by about 0.2 eV. Concerning reduction, the first electron is added to the porphyrin $2e_g(\pi^*)$ orbital in $FeTPP(CO)_2$, again different from the unligated complex. The second electron is also added to $2e_g$ to yield a porphyrin di-anion. The EA of $FeTPP(CO)_2$ is 0.26 eV smaller than that of FeTPP.

In the case of $CoTPP(CO)_2$, the first electron is now abstracted from the metal a_{1g} without electron transfer from metal to ligand. The increase in the energy of a_{1g} leads to a relatively small IP from the orbital. Therefore, solvent coordination to the central metal is able to reduce the oxidation potential of the metal ion and one can expect more facile oxidation to Co^{III}. The first reduction of $CoTPP(CO)_2$ takes place into the porphyrin $2e_g$ although the singly occupied a_{1g} lies lower in energy. The addition of an electron to a_{1g} results in an EA which is nearly 0.8 eV smaller than the EA to $2e_g$. The EA of $CoTPP(CO)_2$ is about 0.6 eV smaller than that of CoTPP.

2. L=HCN

With L=HCN, there is also large upshift in the position of a_{1g}, similar to the L=CO case. With regard to the other valence MOs, however, the electron-donating HCN has an opposite effect to CO, shifting them upward. The exception is $1e_g$, which is lowered in $FeTPP(HCN)_2$ by the weak π backbonding of HCN below the b_{2g}. Note, in contrast, that $1e_g$ is raised in the Co analog, such that π backdonation seems to disappear, consistent with the long $R(\text{Co–N}_{ax})$ and the very small expansion of the equatorial Co–N_{eq} distance. This longer $R(\text{Co–N}_{ax})$ may, in turn, be due to the presence of an electron in the $a_{1g}(\text{M}-d_{z^2})$ orbital in $CoTPP(HCN)_2$. The experimental crystal structure of $CoTPP(piperidine)_2$ shows the same trend in the $\text{Co–N}_{ax/eq}$ bond distance.[66] The calculated $R(\text{Fe–N}_{ax})$ of 1.85 Å is comparable to the $R(\text{Fe–C}_{ax})$ in $FeTPP(CO)_2$. The experimental axial Fe–N bond distance in crystal $FeTPP(piperidine)_2$ is as large as 2.13 Å,[67] probably the consequence of severe steric interactions between piperidine hydrogen and porphinato nitrogen atoms.

The binding energy of $FeTPP–(HCN)_2$ was computed to be 1.0 eV, much smaller than the $FeTPP–(CO)_2$ value. The same is true for $CoTPP–(HCN)_2$ and its CO analog. The weaker binding with the HCN ligands can be attributed to its weaker π backbonding ability. The interactions of the other MTPP species (M=Ni, Cu, Zn) with HCN are extremely weak (0.01 eV) and contain very long M–N_{ax} distances. In these MTPPs, the M-$3d_{z^2}$ is fully occupied, which prevents the close association of any axial ligands.

The first ionization of $FeTPP(HCN)_2$ involves the abstraction of an electron from the porphyrin a_{2u} although the metal b_{2g} and $1e_g$ lie above this orbital. The IP from a_{2u} (6.05 eV) is 0.16 eV smaller than from $1e_g$; the IP from b_{2g} is even larger. It may be anticipated that with a longer separation between the Fe and the HCN ligands, the order of the IPs would revert to that of the unliganded complex, making the IP from a metal orbital the lowest one. It is interesting to note that in $CoTPP(HCN)_2$, the IPs from a_{1g} and a_{2u} are approximately equal and hence one-electron oxidation of the

Downloaded 13 Jun 2011 to 129.123.124.169. Redistribution subject to AIP license or copyright; see http://jcp.aip.org/about/rights_and_permissions

TABLE VII. Calculated properties of metal porphyrins and their fluorinated derivatives.

		M=Fe	M=Co	M=Ni	M=Cu	M=Zn
E_{bind}	MP	10.25	11.01	10.13	7.82	6.52
eV	MPF_4	9.19	9.93	9.02	6.75	5.49
	MTPP	10.07	10.81	9.94	7.63	6.32
	$MTPPF_8$	9.61	10.36	9.55	7.32	6.11
R_{M-N}	MP	1.98	1.98	1.97	2.03	2.06
Å	MPF_4	1.97	1.97	1.97	2.03	2.06
	MTPP	1.97	1.97	1.97	2.03	2.06
	$MTPPF_8$	1.96	1.96	1.98	2.02	2.06
Q_M	MP	0.66	0.59	0.44	0.57	0.63
	MPF_4	0.68	0.61	0.46	0.59	0.64
	MTPP	0.63	0.57	0.42	0.55	0.61
	$MTPPF_8$	0.64	0.59	0.44	0.54	0.64
IP	MP	6.29(a_{1g},first)	6.98(a_{2u})	7.01(a_{1u})	6.96(a_{2u})	6.94(a_{2u})
eV		7.00(a_{2u})	7.08($1e_g$)	7.04(a_{2u})	7.23(b_{1g})	7.93(b_{1g})
				7.26($1e_g$)		
	MPF_4	6.77(a_{1g})(first)	7.04(a_{2u})	7.07(a_{2u})	6.99(a_{2u})	6.96(a_{2u})
		7.03(a_{2u})	7.52($1e_g$)	7.52(a_{1u})	7.58(b_{1g})	8.55(b_{1g})
				7.52($1e_g$)		
	MTPP	5.97(a_{1g})(first)	6.57(a_{2u})	6.59(a_{1u})	6.51(a_{2u})	6.50(a_{2u})
		6.55(a_{2u})	6.72($1e_g$)	6.65(a_{2u})	6.89(b_{1g})	7.42(b_{1g})
					6.91($1e_g$)	
	$MTPPF_8$	6.38(a_{1g})(first)	7.06($1e_g$)	7.16(a_{2u})	7.09(a_{2u})	7.09(a_{2u})
		7.08(a_{2u})	7.12(a_{2u})	7.22(a_{1u})	7.45(b_{1g})	7.63(b_{1g})
				7.23($1e_g$)		
EA	MP	−1.66($1e_g$)	−1.96(a_{1g})	−1.31($2e_g$)	−1.38($2e_g$)	−1.40($2e_g$)
eV				−1.29(b_{1g})	−1.23(b_{1g})	
	MPF_4	−2.07($1e_g$)	−2.43(a_{1g})	−1.83(b_{1g})	−1.76(b_{1g})	−1.74($2e_g$)
				−1.64($2e_g$)	−1.73($2e_g$)	
	MTPP	−1.82($1e_g$)	−2.13(a_{1g})	−1.49($2e_g$)	−1.57($2e_g$)	−1.60($2e_g$)
				−1.41(b_{1g})	−1.34(b_{1g})	
	$MTPPF_8$	−2.32($1e_g$)	−2.69(a_{1g})	−2.17(b_{1g})	−2.22(b_{1g})	−2.09($2e_g$)
	Expt[a]	−2.15±0.15		−1.99($2e_g$)	−2.11($2e_g$)	

[a]Experimental value for $FeTPPF_{20}$ [Ref. 63(a)].

complex may occur at either the metal or ring. In the case of reduction, the situation for L=HCN is the same as for L=CO, except that the calculated EA values are of course quantitatively different.

E. Peripheral substitution

There has been a great deal of interest in substituent effects in porphyrins.[31] For example, some halogenated MTPPs are much more active as catalysts than pure MTPPs. In order to understand this increased catalytic activity, it is necessary to have a detailed understanding of their electronic properties. The effects of *meso*-fluorine and pyrrolic β-fluorine substituents in the MTPPs were addressed here, where the four *meso*-phenyl groups and eight pyrrolic β–H's were replaced by F atoms. Since F is a strongly electron-withdrawing substituent, the multiple substitutions are expected to exert strong electronic effects in the metal porphyrins. The calculated properties of the metal *meso*-tetrafluoroporphyrins MPF_4 and metal β-octafluoroporphyrins $MTPPF_8$ are collected in Table VII, together with the corresponding data of MP and MTPP for comparison. The changes of the orbital levels are illustrated in Fig. 5 for M=Fe and Co.

The first section of data in Table VII illustrates that fluorosubstitution weakens the interaction of each porphyrin with the metal. The magnitude of this binding energy reduction varies from 1 eV for MP to 0.2–0.5 eV for the larger MTPP. Despite this weakening effect, there is very little change observed in the $M-N_{eq}$ bond distances. The presence of the F atoms tends to make the atomic charge on M slightly more positive, by 0.01–0.02.

As is evident in Fig. 5, fluorosubstitution has a lowering effect on most of the molecular orbitals. The magnitude of this shift, surprisingly uniform from one MO to the next, is some 0.4 eV. (The main exceptions are the a_{2u} orbital of FeP, and b_{2u} of FeTPP, which are shifted downward by a much smaller amount). As a result, the ordering of the MOs is left unchanged by the substitution. In general, fluorination effects on the simpler FeP are quite similar to those in FeTPP.

The trends in evidence in Fig. 5 for the Fe complexes are reasonably well reproduced for the other MP complexes. A principal finding in common is the small lowering of the a_{2u} orbital upon fluorosubstitution, confirmed by spectroscopic and electrochemical studies of 2-substituted MTPPs.[68] The near degeneracy of a_{2u} and a_{1u} in MP/MTPP is hence removed upon fluorination. Any variation in the relative energies of a_{2u} and a_{1u} is expected to have significant effects on the physical properties and on reactivities of porphyrins and their π cations.[68] In the cases of M=Co and Ni, for example, the *meso*-tetrafluorination causes the relative order of a_{2u} and $1e_g$ orbitals to reverse.

Corresponding to the downshift of the valence MOs, the

Downloaded 13 Jun 2011 to 129.123.124.169. Redistribution subject to AIP license or copyright; see http://jcp.aip.org/about/rights_and_permissions

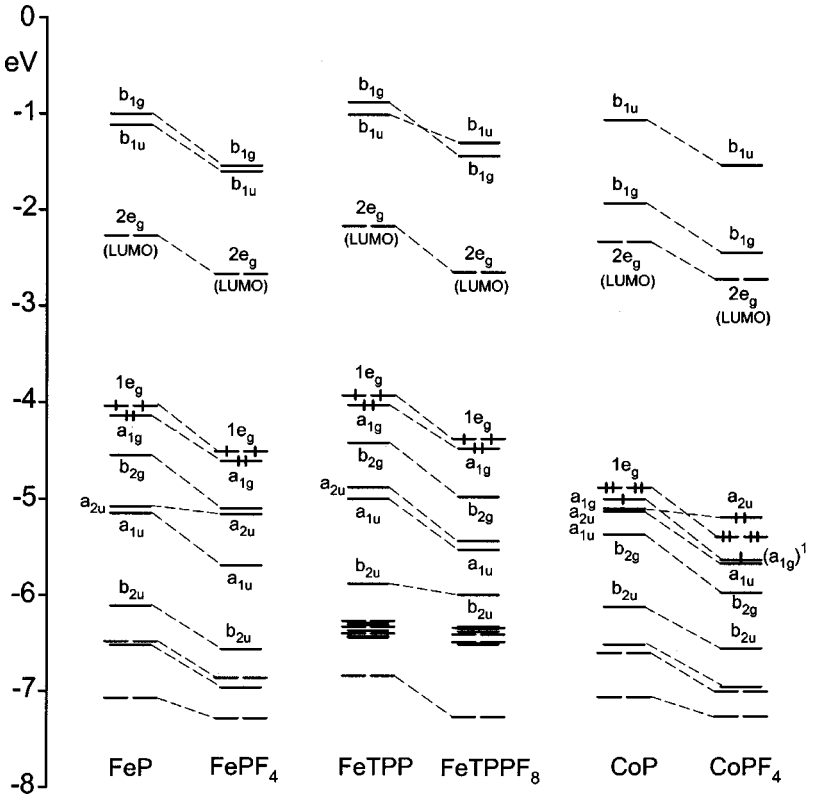

FIG. 5. Orbital energy levels of MP, MPF_4, MTPP, and $MTPPF_8$ for M=Fe and Co.

calculated IPs of $MTPPF_8$ are 0.4–0.6 eV higher than those of MTPP; the IPs of MPF_4 exceed those of MTPP by 0.5–1.0 eV, depending on the metal and particular orbital. Thus the *meso*-substituents exert a stronger effect on the IPs than the same substituents placed in the β-position of the porphyrin. Note that for $CoTPPF_8$, the orbital from which the first ionization takes place is different than that for CoTPP. The same is true for $NiPF_4$ and $NiTPPF_8$. The $[NiPF_4]^+$ cation clearly has a $^2A_{2u}$ ground state because the IP from a_{2u} is 0.5 eV less than that from a_{1u}. $[CoPF_4]^+$ has a ground state of $^3A_{2u}$, 0.13 eV lower than the $^3A_{2g}$ state; there is no longer charge transfer from metal to ligand when the first electron is ionized from a_{2u}. One can also draw the general conclusion that the first IP is reduced by electron-donating substituents such as a phenyl group, while it is increased by electron-withdrawing F, in agreement with the trend in experimental oxidation potentials (E_{12}).[24]

Substituents also exert an effect on electron affinity. As evident in the last section of Table VII, the EA is increased by 0.5–0.7 eV from MTPP to $MTPPF_8$, and by 0.1–0.3 eV from MTPP to MPF_4, which implies that the effect of *meso*-substituents is weaker than that of pyrrolic β-substituents, in contrast to the substituent effect on the IPs. Chen *et al.*[63] have measured gas-phase EAs for some halogenated FeTPPs. The calculated EA value of $FeTPPF_8$ (−2.32 eV) is in good agreement with the experimental value for $FeTPPF_{20}$ (−2.15±0.15 eV). An argument has been proposed that the increase of EA in electron-withdrawing substituted NiTPP suggests significant delocalization of charge into the ligand in the metal porphyrin.[63] According to the calculations on $[NiTPPF_8]^-$ and $[NiPF_4]^-$, however, the unpaired electron in the anion resides in a metal orbital (b_{1g}), different from $[NiTPP]^{-1}$. The stabilization of the b_{1g} orbital is somewhat larger than for $2e_g$. As a result, the orbital that accepts an electron to form the anion is the low-lying metal b_{1g} orbital for the fluorinated Ni and Cu porphyrins.

IV. SUMMARY

(1) The electronic structure of FeTPP is rather complex. The four *3d*-like orbitals (b_{2g},a_{1g},$1e_g$), which are close in energy, generate three low-lying triplets in the energy range of 0–0.3 eV, and a fourth at 0.7 eV. The D_{4h} structure has a $^3A_{2g}$ ground state which arises from the configuration $(d_{xy})^2(d_{z^2})^2(d_{xz})^1(d_{yz})^1$, in agreement with experimental

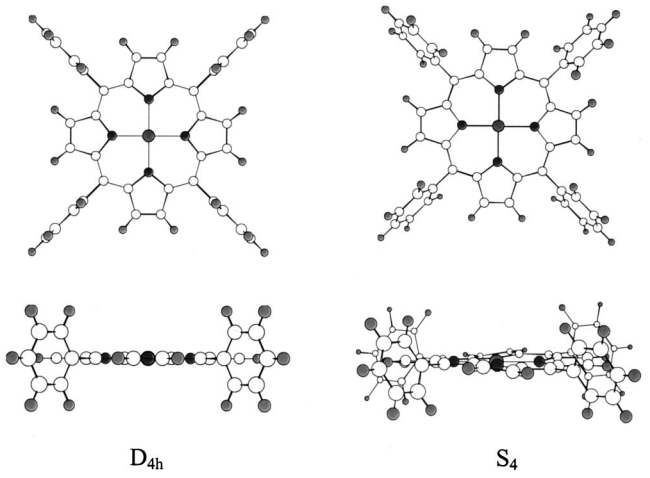

FIG. 6. Different optimized structures of NiTPP; D_{4h} structure top-view (upper part) and side-view (lower part), S_4 structure top-view and side-view.

Downloaded 13 Jun 2011 to 129.123.124.169. Redistribution subject to AIP license or copyright; see http://jcp.aip.org/about/rights_and_permissions

TABLE VIII. Comparison of the calculated properties[a] of NiTPP between the optimized D_{4h} and S_4 (C_2) structures.

	R_{Ni-N}	E_{bind}	IP_1	IP_2	IP_3	IP_4	IP_5	EA
D_{4h}	1.97	9.94	6.59(a_{2u})	6.65(a_{1u})	6.91($1e_g$)	7.46(a_{1g})	7.48(b_{2u})	1.49
S_4	1.95	9.99	6.57	6.64	6.92	7.56	7.48	1.47
$\Delta(S_4-D_{4h})$	−0.02	0.05	−0.02	−0.01	0.01	0.10	0.00	−0.02

[a]Ni–N bond length R in Å, Ni–TPP binding energy E in eV, ionization potentials IP for the outer MOs in eV, electron affinity EA in eV.

measurements,[44–47–50] but differs from prior *ab initio*[7,8,10] calculations. The order of the five lowest states is calculated to be $^3A_{2g}<{}^3E_g(A)<{}^3B_{2g}<{}^3E_g(B)<{}^5A_{1g}$. Our calculations also support the ground state assignment of CoTPP as $(d_{z^2})^1(d_{xz})^2(d_{yz})^2$, or $^2A_{1g}$, 0.2 eV more stable than ^2E_g.

(2) The porphyrin MOs are interspersed with the *d* orbitals of the central metal atom. The HOMOs in Fe, Co, Ni, and Cu are metal 3d-like, whereas in Zn, the HOMO is localized on the porphyrin ring. The energies of the M-*d* orbitals tend to go down along the series, particularly b_{1g}, which sees the contribution of $3d_{x^2-y^2}$ to this orbital drop to as low as 18%.

(3) Oxidation does not necessarily occur from a HOMO in each case. The first oxidation of FeTPP and CoTPP occurs at the central metal, in contrast to the ligand oxidation in the Ni, Cu, and Zn analogies. [The ground state of $[CoTPP]^+$ does not correspond to the state of the first IP which arises from the porphyrin a_{2u} (π) orbital.] The first IPs for CoTPP to ZnTPP are similar and significantly larger than that of FeTPP. There seems to be no obvious correlation between the first IPs and electrochemical oxidation potentials; the latter show substantial variation with the central metal.[28] The second oxidation occurs at the ligand in all cases.

(4) The first reduction in FeTPP and CoTPP occurs at the metal because M has low-lying half-filled *3d*-like orbitals. In the other MTPPs, the site of electron addition is the ring ligand. Predictions arising here concerning the ground states of a series of $[MTPP]^{x-}$ ions allow understanding of a number of observed electronic properties.

(5) There is significant covalency in MTPP, such that the charges assigned to the metal atoms are quite a bit smaller than +2. The metal atoms are strongly bound to the ring in these complexes, with M–TPP binding energies in the range of 6–11 eV. The trend in the binding energies parallels the M–N bond distances that vary significantly with $3d_{x^2-y^2}$ occupation.

(6) Electronic structures are subject to the influence of axial ligands (L). Axial coordination to the square-planar complex results in destabilization of the a_{1g} orbital through σ-bonding interactions. The calculated large binding energy between FeTPP and two L's is in accord with the fact that iron porphyrins have high affinity for additional axial ligands. Thus, the addition of axial ligands can easily make iron porphyrins diamagnetic. CoTPP has a much weaker attraction for axial ligands owing to the unpaired electron located in the d_{z^2} orbital. The sites of oxidation in $FeTPP(L)_2$ and $CoTPP(L)_2$ are dependent on the ligand field strength of L.

(7) F substituents at the β-pyrrole position of the porphyrin systematically cause a downshift in all valence MOs. In contrast, the effect of *meso*-tetrafluoration has only a small apparent influence on the a_{2u} orbital with respect to the other valence MO levels.

(8) The use of MP as a model for larger and more complicated systems is justified, provided suitable caution is exercised. Many electronic properties of the metal porphyrins are insensitive to the presence of phenyl groups. Four phenyl groups added to MP changes the valence IPs by 0.3–0.5 eV, while the EA is altered by some 0.2 eV. The ordering and relative positions of the outer MO levels in MP and MTPP are the same. For many anions, however, the porphine–phenyl interaction can result in different ground states, and the *meso*-tetraphenyl substitution leads to considerably lower EAs for $[MTPP]^{x-}$.

ACKNOWLEDGMENT

This work was supported by Grant No. DAAD19-99-1-0206 from the Army Research Office.

APPENDIX: DIFFERENT OPTIMIZED STRUCTURES OF NiTPP AND COMPARISON BETWEEN THEIR CALCULATED PROPERTIES

See Fig. 6 and Table VIII.

[1] D. Dolphin and R. H. Felton, Acc. Chem. Res. **7**, 26 (1974).
[2] *The Porphyrins*, edited by D. Dolphin (Academic, New York, 1978), Vols. I–VII.
[3] For a review of semiempirical calculations on porphyrins, see M. Gouterman, in *The Porphyrins*, Vol. III, edited by D. Dolphin (Academic, New York, 1978), Vol. III, p. 1–165.
[4] J. Almlöf, Int. J. Quantum Chem. **8**, 915 (1974).
[5] D. Spangler, R. McKinney, R. E. Christoffersen, M. G. Maggiora, and L. L. Shipman, Chem. Phys. Lett. **36**, 427 (1975); D. Spangler, M. G. Maggiora, L. L. Shipman, and R. E. Christoffersen, J. Am. Chem. Soc. **99**, 7470 (1977); **99**, 7478 (1977).
[6] H. Kashiwagi, T. Takada, S. Obara, E. Miyoshi, and K. Ohno, Int. J. Quantum Chem. **14**, 13 (1978).
[7] H. Kashiwagi and S. Obara, Int. J. Quantum Chem. **20**, 843 (1981).
[8] A. Dedieu, M.-M. Rohmer, and A. Veillard, Adv. Quantum Chem. **16**, 43 (1982).
[9] M.-M. Rohmer, Chem. Phys. Lett. **116**, 44 (1985).
[10] D. C. Rawlings, M. Gouterman, E. R. Davidson, and D. Feller, Int. J. Quantum Chem. **28**, 773 (1985).
[11] Y.-K. Choe, T. Nakajima, and K. Hirao, J. Chem. Phys. **111**, 3837 (1999).
[12] D. E. Ellis and Z. Berkovitch-Yellin, J. Chem. Phys. **74**, 2427 (1981).
[13] D. A. Case and M. Karplus, J. Am. Chem. Soc. **99**, 6182 (1977); S. F. Sontum, D. A. Case, and M. Karplus, J. Chem. Phys. **79**, 2881 (1983).
[14] W. D. Edwards, B. Weiner, and M. C. Zerner, J. Am. Chem. Soc. **108**, 2196 (1986).
[15] B. Delley, Physica B **172**, 185 (1991).
[16] D. H. Jones, A. S. Hinman, and T. Ziegler, Inorg. Chem. **32**, 2092 (1993).
[17] A. Rosa and E. J. Baerends, Inorg. Chem. **32**, 5637 (1993).
[18] N. Matsuzawa, M. Ata, and D. A. Dixon, J. Phys. Chem. **99**, 7698 (1995).
[19] D. Lamoen and M. Parrinello, Chem. Phys. Lett. **248**, 309 (1996).

Downloaded 13 Jun 2011 to 129.123.124.169. Redistribution subject to AIP license or copyright; see http://jcp.aip.org/about/rights_and_permissions

[20] P. M. Kozlowski, T. G. Spiro, A. Bérces, and M. Z. Zgierski, J. Phys. Chem. B **102**, 2603 (1998).
[21] A. B. P. Lever and J. P. Wilshire, Can. J. Chem. **54**, 2514 (1976).
[22] G. L. Closs and L. E. Closs, J. Am. Chem. Soc. **85**, 818 (1963).
[23] J. W. Dodd and N. S. Hush, J. Chem. Soc. **1964**, 4607; N. S. Hush and D. W. Clack, J. Am. Chem. Soc. **87**, 4238 (1965); N. S. Hush and J. R. Rowlands, *ibid.* **89**, 2976 (1967).
[24] P. Cocolios and K. M. Kadish, Isr. J. Chem. **25**, 138 (1985).
[25] A. Wolberg and J. Manassen, J. Am. Chem. Soc. **92**, 2982 (1970).
[26] K. K. Irikura and J. L. Beauchamp, J. Am. Chem. Soc. **113**, 2767 (1991).
[27] Y. Niwa, J. Chem. Phys. **62**, 737 (1975).
[28] J.-H. Fuhrhop, K. M. Kadish, and D. G. Davis, J. Am. Chem. Soc. **95**, 5140 (1973).
[29] K. Takahashi, T. Komura, and H. Imanaga, Bull. Chem. Soc. Jpn. **62**, 386 (1989).
[30] C. H. Langford, S. Seto, and B. R. Hollebone, Inorg. Chim. Acta **90**, 221 (1984).
[31] P. G. Gassman, A. Ghosh, and J. Almlöf, J. Am. Chem. Soc. **114**, 9990 (1992); A. Ghosh and J. Almlöf, Chem. Phys. Lett. **213**, 519 (1993); A. Ghosh, J. Phys. Chem. **98**, 11004 (1994); J. Am. Chem. Soc. **117**, 4691 (1995); Acc. Chem. Res. **31**, 189 (1998).
[32] ADF program package, version 2.0.1: E. J. Baerends, D. E. Ellis, and P. Ros, Chem. Phys. **2**, 41 (1973); G. te Velde and E. J. Baerends, J. Comput. Phys. **99**, 84 (1992).
[33] T. Ziegler, V. Tschinke, E. J. Baerends, J. G. Snijders, and W. Ravenek, J. Phys. Chem. **93**, 3050 (1989).
[34] S. H. Vosko, L. Wilk, and M. Nusair, Can. J. Phys. **58**, 1200 (1980).
[35] A. D. Becke, Phys. Rev. A **38**, 3098 (1988).
[36] J. P. Perdew, Phys. Rev. B **33**, 8822 (1986).
[37] B. G. Johnson, P. M. W. Gill, and J. A. Pople, J. Chem. Phys. **98**, 5612 (1993); J. Li, G. Schreckenbach, and T. Ziegler, J. Am. Chem. Soc. **117**, 486 (1995).
[38] R. Stowasser and R. Hoffmann, J. Am. Chem. Soc. **121**, 3414 (1999); G. Papoian, J. K. Norskov, and R. Hoffmann, *ibid.* **122**, 4129 (2000).
[39] W. Jentzen, I. Turowska-Tyrk, W. R. Scheidt, and J. A. Shelnutt, Inorg. Chem. **35**, 3559 (1996).
[40] M. P. Byrn, C. J. Curtis, Y. Hsiou, S. I. Khan, P. A. Sawin, S. K. Tendick, A. Terzis, and C. E. Strouse, J. Am. Chem. Soc. **115**, 9480 (1993).
[41] A. L. Maclean, G. J. Foran, B. J. Kennedy, P. Turner, and T. W. Hambley, Aust. J. Chem. **49**, 1273 (1996).
[42] D. P. Piet, D. Danovich, H. Zuilhof, and E. J. R. Sudhölter, J. Chem. Soc., Perkin Trans. 2 **1999**, 1653.
[43] T. S. RushIII, P. M. Kozlowski, C. A. Piffat, R. Kumble, M. Z. Zgierski, and T. G. Spiro, J. Phys. Chem. B **104**, 5020 (2000).
[44] J. P. Collman, J. L. Hoard, N. Kim, G. Lang, and C. A. Reed, J. Am. Chem. Soc. **97**, 2676 (1975).
[45] P. Madura and W. R. Scheidt, Inorg. Chem. **15**, 3182 (1976).
[46] E. B. Fleischer, C. K. Miller, and L. E. Webb, J. Am. Chem. Soc. **86**, 2342 (1964).
[47] H. Goff, G. N. La Mar, and C. A. Reed, J. Am. Chem. Soc. **99**, 3641 (1977).
[48] G. Lang, K. Spartalian, C. A. Reed, and J. P. Collman, J. Chem. Phys. **69**, 5424 (1978).
[49] P. D. W. Boyd, A. D. Buckingham, R. F. McMecking, and S. Mitra, Inorg. Chem. **18**, 3585 (1979).
[50] J. Mispelter, M. Momenteau, and J. M. Lhoste, J. Chem. Phys. **72**, 1003 (1980).
[51] C. Weiss, H. Kobayashi, and M. Gouterman, J. Mol. Spectrosc. **16**, 415 (1965).
[52] J. S. Griffith, Discuss. Faraday Soc. **26**, 81 (1958); M. Sato, H. Kon, H. Akoh, A. Tasaki, C. Kabuto, and J. V. Silverton, Chem. Phys. **16**, 405 (1976).
[53] W. C. Lin, Inorg. Chem. **15**, 1114 (1976).
[54] R. H. Felton and H. Linschitz, J. Am. Chem. Soc. **88**, 1113 (1966).
[55] J. Subramanian, in *Porphyrins and Metallopophyrins*, edited by K. M. Smith (Elsevier Scientific, Amsterdam, 1975), p. 555.
[56] J. Fajer, D. C. Borg, A. Forman, A. D. Adler, and V. Varadi, J. Am. Chem. Soc. **96**, 1238 (1974).
[57] S. C. Khandelwal and J. L. Roebber, Chem. Phys. Lett. **34**, 355 (1975).
[58] Y. Nakato, K. Abe, and H. Tsubomura, Chem. Phys. Lett. **39**, 358 (1976).
[59] L. J. Boucher and J. J. Katz, J. Am. Chem. Soc. **89**, 1340 (1967).
[60] S. Kitagawa, I. Morishima, T. Yonezawa, and N. Sato, Inorg. Chem. **18**, 1345 (1979).
[61] P. Dupuis, R. Roberge, and C. Sandorfy, Chem. Phys. Lett. **75**, 434 (1980).
[62] S. J. Silvers and A. Tulinsky, J. Am. Chem. Soc. **89**, 3331 (1967).
[63] H. L. Chen, P. E. Ellis, Jr., T. Wijesekera, T. E. Hagan, S. E. Groh, J. E. Lyons, and D. P. Ridge, J. Am. Chem. Soc. **116**, 1086 (1994); H. L. Chen, Y. H. Pan, S. Groh, T. E. Hagan, and D. P. Ridge, *ibid.* **113**, 2766 (1991).
[64] G. N. La Mar and F. A. Walker, J. Am. Chem. Soc. **95**, 1790 (1973).
[65] S.-M. Peng and J. A. Ibers, J. Am. Chem. Soc. **98**, 8032 (1976).
[66] W. R. Scheidt, J. Am. Chem. Soc. **96**, 84 (1974).
[67] L. J. Radonovich, A. Bloom, and J. L. Hoard, J. Am. Chem. Soc. **94**, 2073 (1972).
[68] R. A. Binstead, M. J. Crossley, and N. S. Hush, Inorg. Chem. **30**, 1259 (1991).

Downloaded 13 Jun 2011 to 129.123.124.169. Redistribution subject to AIP license or copyright; see http://jcp.aip.org/about/rights_and_permissions